

COBRA: A Computational Brewing Application for Predicting the Molecular Composition of Organic Aerosols

David R. Fooshee,^{‡,†} Tran B. Nguyen,^{§,†} Sergey A. Nizkorodov,^{*,§} Julia Laskin,^{||} Alexander Laskin,[⊥] and Pierre Baldi^{*,‡}

[‡]School of Information and Computer Sciences, University of California, Irvine, California 92697-3435, United States

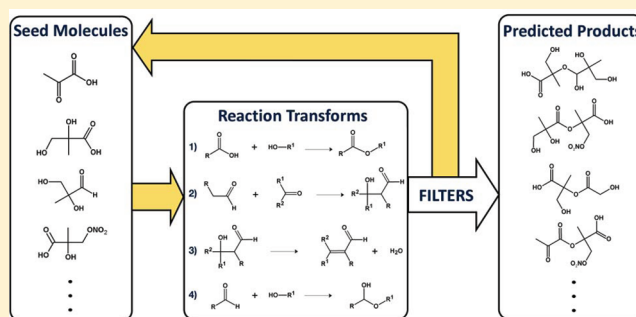
[§]Department of Chemistry, University of California, Irvine, California 92697-2025, United States

^{||}Chemical and Materials Sciences Division, Pacific Northwest National Laboratory, Richland, Washington 99352, United States

[⊥]Environmental Molecular Sciences Laboratory, Pacific Northwest National Laboratory, Richland, Washington 99352, United States

S Supporting Information

ABSTRACT: Atmospheric organic aerosols (OA) represent a significant fraction of airborne particulate matter and can impact climate, visibility, and human health. These mixtures are difficult to characterize experimentally due to their complex and dynamic chemical composition. We introduce a novel Computational Brewing Application (COBRA) and apply it to modeling oligomerization chemistry stemming from condensation and addition reactions in OA formed by photo-oxidation of isoprene. COBRA uses two lists as input: a list of chemical structures comprising the molecular starting pool and a list of rules defining potential reactions between molecules. Reactions are performed iteratively, with products of all previous iterations serving as reactants for the next. The simulation generated thousands of structures in the mass range of 120–500 Da and correctly predicted ~70% of the individual OA constituents observed by high-resolution mass spectrometry. Select predicted structures were confirmed with tandem mass spectrometry. Esterification was shown to play the most significant role in oligomer formation, with hemiacetal formation less important, and aldol condensation insignificant. COBRA is not limited to atmospheric aerosol chemistry; it should be applicable to the prediction of reaction products in other complex mixtures for which reasonable reaction mechanisms and seed molecules can be supplied by experimental or theoretical methods.



1. INTRODUCTION

Atmospheric organic aerosols (OA), airborne particles comprised primarily of organic material, are estimated to contribute up to 50% of the total particulate matter mass at continental midlatitudes and up to 90% at forested areas.¹ OA impact climate and visibility by interacting with solar radiation, atmospheric oxidants, and water vapor² and are associated with adverse effects on human health as discussed in ref 3 and references therein. The climate, visibility, and health effects of OA are dependent on their chemical composition.^{4–6} However, the diversity of OA formation and growth mechanisms makes detailed molecular chemical composition of OA difficult to predict by traditional modeling or characterize by experimental methods. During their residence time in the atmosphere, OA undergo chemical aging processes^{7,8} that further enhance molecular complexity through, for example, the formation of nitrogen-containing organic compounds (NOC).^{9–11}

Recent advances in high-resolution mass spectrometry (HR-MS) have enabled simultaneous detection of hundreds of individual molecules in OA.^{9,12–15} HR-MS tools are useful in providing the molecular formulas for OA constituents. Ion fragmentation patterns observed in tandem mass spectrometry

(MSⁿ) experiments provide additional information about the structures. However, interpretation of MSⁿ data is complicated by the presence of multiple structural isomers and lack of sufficiently diagnostic fragmentation patterns. In previous work, reliable structural information could only be extracted for the low molecular weight (MW) species^{16,17} and homologous oligomers^{18–20} present in OA, leaving the structures of the majority of complex oligomers uncharacterized.

HR-MS experiments suggest that in many cases, oligomeric compounds in atmospheric OA are produced from repetitive reactions between the OA constituents.^{17,20–22} There is strong evidence that condensation reactions such as esterification and aldol condensation^{18,20,23–28} and addition reactions such as hemiacetal formation^{29–31} are quite common in both organic aerosols and in aqueous solutions of OA. Advanced computational approaches are needed for predicting the OA composition using a bottom-up approach, in which the starting

Received: February 1, 2012

Revised: May 1, 2012

Accepted: May 8, 2012

Published: May 8, 2012

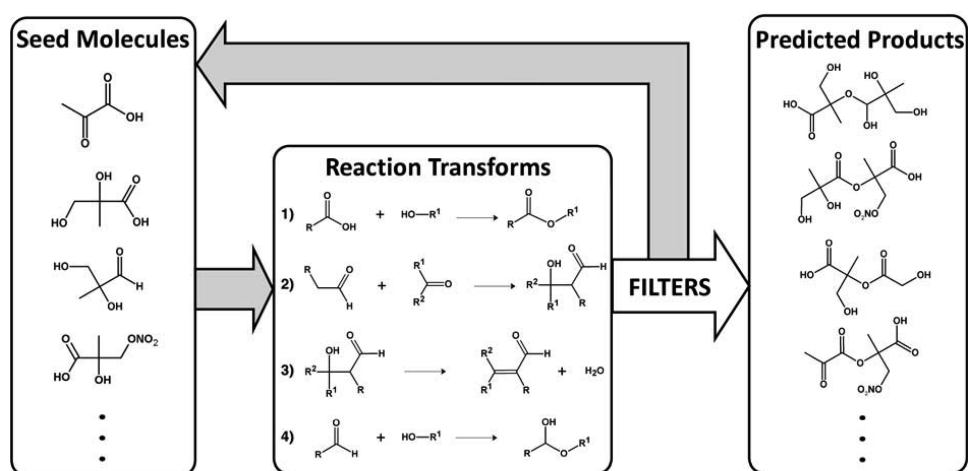


Figure 1. A schematic representation of COBRA. COBRA converts a set of seed molecules into a set of predicted products using predefined chemical reaction rules. This process is repeated for several iterations, with predicted products going back into the pool of reacting molecules after each step. The four reactions used in this work are shown in the center panel, and the full list of 27 seed molecules is shown in Table 1.

low-molecular weight compounds are known from experiments, and reaction rules for combining these compounds into oligomers can be unambiguously defined.

This work describes the first application of a Computational Brewing Application (COBRA) to modeling oligomerization products observed in the detailed composition of OA. Figure 1 shows a diagrammatic representation of COBRA, which is a customizable simulation engine for chemical reactions. Prior work from our group related to predicting the mechanisms of organic chemical reactions has focused on a rule-based approach with broad knowledge of general organic chemistry³² or a machine learning approach to reaction prediction based on ranking mechanistic steps by productivity.³³ COBRA differs from these approaches in that it is optimized to simulate the evolution of a complex mixture by combinatorial computation of many thousands of chemical reactions between mixture constituents, based on a chosen pool of starting (seed) compounds and specific reaction mechanisms. For the case study presented in this work, the formation of a large set of experimentally observed high-MW oligomeric products in OA derived from the photooxidation of isoprene^{20,22} is modeled by considering chemical transformations of a basic set of monomers through the following oligomerization reactions: esterification, aldol condensation, and hemiacetal formation. We demonstrate that COBRA succeeds at modeling relevant oligomerization chemistry, predicting and visualizing high-MW compound structures, and predicting unique reaction products in OA. More broadly, the COBRA approach is applicable to studying the evolution of a wide range of organic mixtures as long as the starting components and reaction mechanisms can be suggested.

2. METHODS

2.1. COBRA. Chemical structures are input into COBRA using the widely used chemical string representation SMILES.³⁴ Reaction transforms are defined using the reaction transform language SMIRKS.³⁵ The SMIRKS language is a superset of SMILES and can be used to define reaction transforms to an arbitrary degree of specificity. We leverage the programming language Python in conjunction with OpenEye's OEChem library³⁶ to process the input SMILES and SMIRKS into predicted products. Standard valence rules are explicitly

programmed into the reaction transforms in order to predict chemically meaningful structures. Specifically, R-groups in the reactions shown in Figure 1 were allowed to be alkyl or acyl groups but not hydrogen alone. Filters can be imposed to prevent compounds with certain properties from participating in reactions or from being included in the pool of final products.

The simulation includes the following iterative steps. 1) For each molecule and each pair of molecules in the reactant pool, all unimolecular reaction transforms and all bimolecular transforms, respectively, are applied. Identical reactions already performed in the previous iterations are recognized and skipped. 2) The product molecules are filtered. For this simulation, we automatically filter out any molecule with greater than 40 heavy (C, O, N) atoms. This filter restricts the molecular weights of the products below approximately 500 Da, the limit at which molecular assignments made with 0.1 mDa accuracy can be uniquely determined for $C_cH_hO_oN_nS_s$ species.³⁷ This restriction significantly decreased the model run time while still capturing the chemistry of the most abundant compounds in isoprene high-NO_x SOA.²² 3) Molecules that were not filtered out during the previous step are added back into the reactant pool, and the system returns to step one. The simulation is complete either after the requested number of iterations has passed or after a specified number of unique reactions has been simulated (30,000 reactions for the full simulation and the exclusion simulations, in this study). Results can then be conveniently visualized and searched for specific chemical structures matching any specified structural criteria. Additionally, we can compute the sequence of reactions that led to a given product's formation.

2.2. Experimental Methods. Isoprene OA was photochemically generated in a 5 m³ Teflon chamber, as described previously.²⁰ Samples were generated in dry air, under high-NO_x (VOC:NO_x <1) conditions and in the absence of inorganic seed particles. H₂O₂ was used as an OH precursor. The initial mixing ratio of isoprene was 250 ppbv (parts per billion by volume). Blank samples were produced in an identical manner as OA samples, without UV radiation. Samples were collected on Teflon filters (0.2 μm pore size, Millipore), vacuum sealed, and frozen prior to analysis. Negative ion mode direct injection ESI (tip voltage 4 kV)

Table 1. Seed Molecules Used for the COBRA Simulations Described in This Work

Formula	Name	Structure	Formula	Name	Structure
C ₂ H ₄ O ₂	glycolaldehyde		C ₄ H ₈ O ₄	2-methylglyceric acid	
C ₂ H ₄ O ₂	acetic acid		C ₄ H ₈ O ₄	erythrose/threose	
C ₂ H ₄ O ₃	glycolic acid		C ₄ H ₆ O ₄	methylmalonic acid	
C ₃ H ₄ O ₂	methylglyoxal		C ₄ H ₆ O ₄	2-hydroxy-2-methyl-3-oxopropanoic acid	
C ₃ H ₄ O ₂	acrylic acid		C ₄ H ₆ O ₅	hydroxy(methyl)propanedioic acid	
C ₃ H ₆ O ₂	hydroxyacetone		C ₄ H ₇ O ₆ N	2-methylglyceric acid 3-nitrate	
C ₃ H ₆ O ₂	propanoic acid		C ₄ H ₈ O ₅	2,3,3-trihydroxy-2-methylpropanoic acid	
C ₃ H ₄ O ₃	pyruvic acid		C ₅ H ₈ O ₃	2-hydroxy-2-methylbutanedial	
C ₃ H ₆ O ₃	lactic acid		C ₅ H ₈ O ₄	methylsuccinic acid	
C ₃ H ₄ O ₄	3-hydroxypyruvic acid		C ₅ H ₈ O ₄	2-hydroxy-2-Me-4-oxobutanoic acid	
C ₃ H ₄ O ₄	2-hydroxy-3-oxopropanoic acid		C ₅ H ₈ O ₅	2-hydroxy-2-methylbutanedioic acid	
C ₄ H ₆ O ₂	methacrylic acid		C ₅ H ₁₀ O ₃	2,4-dihydroxy-2-methylbutanal	
C ₄ H ₆ O ₃	2-methyloxopropanoic acid		C ₅ H ₁₀ O ₅	2,3,4-trihydroxy-2-Mebutanoic acid	
C ₄ H ₈ O ₃	2-methylglyceraldehyde				

was used as an ionization method for solvent-extracted OA samples. The solvents used for analysis were water and acetonitrile (both HPLC grade, Fluka) at a 1:1 volume ratio. Mass analysis was done with a high-resolution linear ion trap (LTQ-) Orbitrap (Thermo Corp.) at Pacific Northwest National Lab (PNNL) Environmental Molecular Science Laboratory facility (EMSL), with a mass resolution of 60,000 $m/\Delta m$ at m/z 400. MS^n studies were performed in the LTQ, with mass selection in the 0.5 m/z range and collision-induced-dissociation energies of 20–40 energy units. Product ions of MS^n were analyzed in the Orbitrap.

3. RESULTS AND DISCUSSION

Table 1 lists the seed molecules for the simulation. These low-MW species have been identified as important building blocks in the formation of isoprene photooxidation OA.²² The majority of these molecules have been detected in isoprene OA (ref 38 and references therein) and are primarily multifunctional carbonyl, alcohol, and carboxyl compounds derived from the oxidation of isoprene with the hydroxyl radical (OH).^{18,22,39–46} Some of these molecules have sufficiently high vapor pressure to exist primarily in the gas phase. For example,

glycolaldehyde has a room temperature vapor pressure of 0.028 Torr⁴⁷ and may participate in aerosol mass-growth reactions initiated in the gas- or heterogeneous phase. Note that glyoxal is not included among the seed molecules used in these simulations because it was not found among the monomer units inferred from mass spectrometry of isoprene oxidation products as described in ref 22. The 3-nitrate ester of 2-methylglyceric acid (2MGA)^{18,20,27,45} represents the sole NOC in the list of seed molecules. Available information about NOC monomers is limited due to the small number of studies of NOC composition in the literature (ref 22 and references therein).

COBRA was used to simulate the evolution of a virtual OA mixture by applying the four reaction transforms shown in Figure 1 to the set of 27 starting molecules in Table 1. The resulting product pool contained 135,107 predicted structures after performing 30,000 unique reactions, representing a total of 758 unique elemental formulas of the type C_cH_hO_oN_n with MW < 500 Da. The 2 orders of magnitude difference between the number of structures and elemental formulas reflects a large number of predicted structural isomers. The experimental HR-MS data from ref 22 (Table S1 in the Supporting Information)

contains 464 neutral elemental formulas, and 323 of these formulas (70%) were predicted by COBRA. Figure 2 shows the

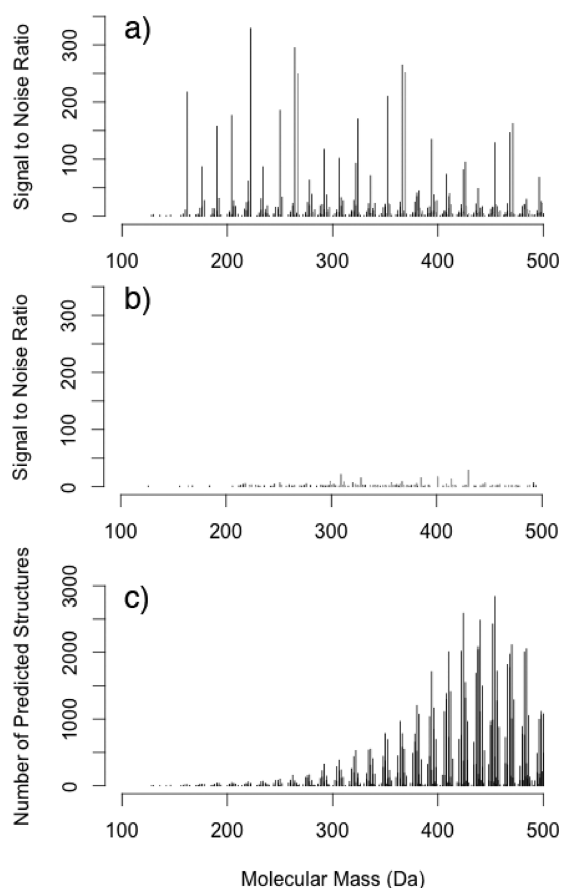


Figure 2. Comparison between the HR-MS experiment and COBRA predictions. Panel (a) shows the HR-MS peaks that are predicted by COBRA (70%). Panel (b) shows the remaining 30% of HR-MS peaks that are not predicted by our simulation. In both panels, NOC peaks are colored green. Panel (c) indicates the number of isomeric structures predicted at each observed molecular mass.

experimental HR-MS spectrum separated into two panels. The first panel shows all HR-MS peaks in the experimental spectrum that were predicted by COBRA (Figure 2A), and the second one shows peaks that did not appear in the COBRA output (Figure 2B). As Figure 2 demonstrates, the 70% fraction of the experimentally observed peaks predicted by COBRA represents the most abundant compounds with MW < 500 Da. The remaining 30% fraction has average peak intensities that are more than an order of magnitude smaller compared to the average peak intensities associated with the successfully

predicted compounds, suggesting that COBRA captures the essential chemistry producing oligomers in isoprene high-NOx OA. The high degree of overlap between the predicted and observed formulas confirms that the oxygenated hydrocarbon seed molecules proposed in our previous work are the relevant oligomer building blocks in this type of OA.²² The fact that a relatively small set of modeled reactions was sufficient to account for roughly 70% of the HR-MS peaks suggests that the oligomerization chemistry in isoprene OA is well constrained.

The fraction of the experimentally observed compounds that are correctly predicted by the simulation can be a misleading metric of success in some cases. For example, if the simulation were significantly overdefined, and generated every possible $C_cH_hO_oN_n$ formula ($\sim 10^5$) allowed by the valence rules, this fraction would become 100%. Therefore the reverse comparison of the fraction of predicted peaks that show up in the experiment is just as important. In the present case, 43% of predicted formulas correspond to compounds detected by HR-MS, and the remaining 57% are not observed. This level of agreement can be viewed as good, considering that the simulation does not use any kinetics restrictions and predicts the formation of compounds that may be below the limit of detection of HR-MS.

It is remarkable that a total of 62 NOC molecular formulas were predicted stemming from 2MGA-3-nitrate alone, representing 41% of the total NOC observed in the isoprene OA sample in the m/z 120–500 range (Figure 2A). Note that this particular simulation's ability to predict NOC compounds is limited because only a single NOC seed molecule is included. Nonetheless, the data confirm that 2MGA-3-nitrate is a prolific oligomer building block in isoprene OA that produces a variety of products through oligomerization in the condensed phase.^{18,20,27,45}

Since structural complexity increases with molecular size, the number of structural and stereo isomers that can be produced by oligomerization reactions also grows exponentially with increasing mass of the individual products (Figure 2C). For the 323 experimentally observed molecular formulas, COBRA predicts 102,650 unique structures, with the number of isomers ranging from 1 to nearly 3,000. The apparent decrease in the number of hits as MW approaches 500 Da is a result of filtering; we artificially limit structures in the product pool to those with less than 40 heavy atoms and do not consider structures with molecular weights in excess of 500 Da. Despite the large number of predicted isomers, the simulation results help constrain possible structures, especially for lower-MW compounds. For example, over 1,000 unique molecular structures associated with a molecular mass of 142.063 Da, assigned to $C_7H_{10}O_3$, can be retrieved from Internet-based chemical inventories (e.g., SciFinder). In contrast, COBRA

Table 2. Small Fraction of the Full Output from COBRA^a

product mass (Da)	product formula	hits (n)	SMILES # 1	SMILES # 2	SMILES # n
128.047	$C_6H_8O_3N_0$	4	<chem>CC(=C)C(=O)OCC=O</chem>	<chem>CC(=C)C(=O)OC(=O)C</chem>	<chem>CC(=O)COC(=O)C=C</chem>
130.027	$C_5H_6O_4N_0$	4	<chem>CC(=O)C(=O)OCC=O</chem>	<chem>CC(=O)C(=O)OC(=O)C</chem>	<chem>C=CC(=O)OCC(=O)O</chem>
132.042	$C_5H_8O_4N_0$	9	<chem>CCC(=O)OC(=O)CO</chem>	<chem>CCC(=O)OCC(=O)O</chem>	<chem>CC(C(=O)O)OC(=O)C</chem>
136.037	$C_4H_8O_3N_0$	2	<chem>C(C(O)OC(=O)CO)O</chem>	<chem>C(C(O)OCC(=O)O)O</chem>	
142.063	$C_7H_{10}O_3N_0$	2	<chem>CCC(=O)OC(=O)C(=C)C</chem>	<chem>CC(=C)C(=O)OCC(=O)C</chem>	
146.022	$C_5H_6O_5N_0$	8	<chem>CC(=O)C(=O)OC(=O)CO</chem>	<chem>CC(=O)C(=O)OCC(=O)O</chem>	<chem>CC(=O)OC(C=O)C(=O)O</chem>

^aFor each observed product, several different isomers (SMILES structures) are predicted (number of hits). The full number of hits for each mass is shown in Figure 2C.

predicts only two structures of $C_7H_{10}O_3$, thereby dramatically reducing the complexity (Table 2). This represents more than a one hundred-fold increase in the level of confidence in assigning molecular structures to a given formula obtained by HR-MS. Even at high masses, COBRA predictions remain useful because the structural information for high-MW compounds is not readily available from chemical databases, and this type of modeling is a practical step toward understanding the possible structures of large oligomers.

A few published studies used MS^n fragmentation data to determine structures of the oligomers in isoprene high-NO_x SOA.^{18,19,22} All molecular structures described in the previous studies match structures predicted by COBRA. To further test the validity of the COBRA predictions, we made a comparison to MS^n studies previously performed by our group of NOC oligomers observed in SOA generated from isoprene photo-oxidation.²² Figure 3 shows the predicted structures of two

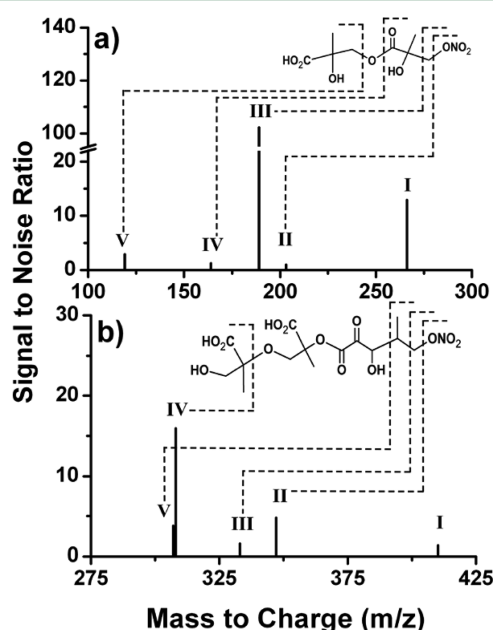


Figure 3. Experimental MS^2 fragmentation spectra for precursor (I) ions (a) $C_8H_{12}NO_9^-$ and (b) $C_{14}H_{20}NO_{13}^-$. Two structures predicted by COBRA that are consistent with the fragmentation patterns are overlaid on the spectra. Product ions are obtained from fragmentation at the dashed bonds (after losses of neutral molecules). Product ions for (a) are as follows: II. m/z 203.056 (I- HNO_3); III. m/z 189.040 (I- CH_3NO_3); IV. m/z 164.020 (I- $C_4H_6O_3$); V. m/z 119.035 (I- $C_4H_5NO_3$). Product ions for (b) are as follows: II. m/z 347.098 (I- HNO_3); III. m/z 333.082 (I- CH_3NO_3); IV. m/z 308.062 (I- $C_4H_6O_3$); V. m/z 307.082 (I- $C_3H_5NO_3$).

NOC oligomers, $C_8H_{13}NO_9$ (267.059 Da) and $C_{14}H_{20}NO_{13}$ (411.101 Da), that are most consistent with MS^n experiments. The MS^n experiments were performed using the negative ion mode; therefore, the molecular masses of the detected compounds are those of deprotonated molecules. Oligomer fragmentation is often characteristic of the functional groups and monomer units present within the compound. For example, HNO_3 and CH_3NO_3 are characteristic MS^n losses from organic nitrates, and $C_4H_6O_3$ is a characteristic loss from the carbonyl ester unit of 2MGA.^{18,22}

For a given molecular formula, the proposed structures based on MS^n experiments described in ref 22 match at least one of the structures predicted by COBRA. We note that structural

isomers may not have distinct fragmentation patterns, and therefore it is possible that the experimental MS^n data represents several structural isomers predicted by COBRA. COBRA predicted four isomeric structures for $C_8H_{13}NO_9$, and at least one predicted structure is consistent with the fragmentation pattern produced by MS^n studies. For $C_{14}H_{21}NO_{13}$, at least one out of 44 predicted structures is consistent with the MS^n fragmentation pattern. Therefore, it is reasonable to hypothesize that other structures predicted by COBRA may be present in the OA, perhaps but not necessarily, in lower quantity than the most abundant isomer.

To elucidate which seed molecules were the most important as oligomer building blocks for isoprene OA, we performed 27 “exclusion” simulations, each with a different seed molecule omitted. Each exclusion simulation was limited to the same number of reactions (30,000). The total number of experimental molecular formulas recovered in each case was compared against a simulation in which no seed molecules were omitted. The “exclusion percent” was calculated as a percent reduction in the number of predicted formulas matching experimental formulas. The highest exclusion percent (19%) was for the 3-nitrate ester of 2-methylglyceric acid, consistent with its special role of being the sole NOC precursor. Specifically, the removal of 2MGA-3-nitrate eliminated all NOC oligomers from the product pool. Removal of other seed molecules resulted in smaller variation in the number of predicted formulas, ranging from -6 to 6%. Note that because of the fixed number of reactions in these simulations, an exclusion of a less significant contributor to chemistry can actually lead to a slight increase in the total number of predicted formulas, yielding a negative exclusion percent. None of the nitrogen-free compounds appeared to stand out from the rest, suggesting some redundancy in the pool of seed molecules. The redundancy in seed molecules lowered the percent overlap between simulation and experiment. These results highlight the need for future work in determining missing precursors and reaction mechanisms. In general, this type of exclusion analysis is useful for assessing the contribution of a single molecule to the total product pool, e.g. the importance of glyoxal in heterogeneous reaction with various OA constituents,^{48–51} or the contribution of first vs second generation VOC oxidation products to producing condensable organic compounds.

We performed additional exclusion simulations, in which one of the four reactions shown in Figure 1 was disabled. The results of the simulations based on the three remaining reactions were compared to the results of the full simulation. Table 3 lists the percent reduction in the number of experimentally observed molecular formulas recovered by the

Table 3. Results from an Exclusion Analysis, in Which One of the Four Reactions Shown in Figure 1 Is Disabled

reaction transform	reaction type	percent reduction in experimentally observed formulas	percent reduction in theoretically predicted formulas	percent reduction in theoretically predicted structures
1	esterification	40.9	12.8	37.8
2	aldol condensation	0.3	0.7	5.6
3	elimination of water from aldol condensates	0	1.5	0.01
4	hemiacetal formation	10.2	-0.1	46.7

simulation, the percent reduction in the number of theoretically predicted molecular formulas, and the percent reduction in the number of theoretically predicted structures generated by the simulation. The esterification reaction (Reaction 1) played the most significant role in recovering experimentally observed formulas, with an exclusion percent of 40.9%, followed by the hemiacetal formation reaction (Reaction 4) with an exclusion percent of 10.2%. The esterification and hemiacetal formation reactions also made the largest contributions to the total number of theoretically predicted structures. Exclusion of esterification from the simulation reduced the number of structures in the COBRA output by 37.8%, while exclusion of hemiacetal formation resulted in a 46.7% decrease. Although hemiacetal formation is prolific at generating theoretical structures, the results demonstrate that esterification is the most important reaction in promoting oligomerization in isoprene OA, while hemiacetal formation is of secondary importance. These results are consistent with a previous study, wherein reducing aerosol liquid water content changed the composition of isoprene high-NO_x SOA most drastically by hindering the esterification reaction.²⁰ They are also consistent with the fast and efficient reactions of OA compounds containing carboxylic acid groups and carbonyls with alcohols observed in ref 52. In contrast, aldol condensation (Reactions 2 and 3) does not appear to play a significant role in forming the oligomers. Removal of either Reaction 2 or Reaction 3 resulted in a small reduction in the number of theoretically produced structures and recovered HR-MS formulas.

Once a pool of COBRA-generated simulation products is available, it can easily be mined for desired products or classes of products. For example, we are interested in the potential for isoprene photooxidation to generate α,β -unsaturated aldehydes, a class of genotoxic compounds found in cigarette smoke and air pollution.^{53–58} The most common atmospheric α,β -unsaturated aldehydes with adverse health effects are gas-phase species such as acrolein (C₃H₄O).⁵⁹ However, adverse health effects are also strongly linked to inhalation of particulate matter,^{3,60–64} which contains more complex and poorly characterized organics. COBRA predicted 6,131 structures corresponding to α,β -unsaturated aldehydes in the isoprene photooxidation SOA data set. This large set of structures can be filtered further, by mass, O/C ratio, or any other property required to yield a focused set of predicted structures. Applying a computational tool like COBRA along with the molecular-level experimental characterization of products is a powerful first step to identifying condensed-phase atmospheric toxins.

One limitation of COBRA is that it does not currently include kinetics information and therefore cannot model the relative abundances of individual products. This limitation may be important in cases where the product branching ratios from a particular reaction are dissimilar or dependent on atmospheric conditions, in which case the results from COBRA will artificially enhance the importance of noncompetitive products. For example, in the absence of nitrogen oxides (NO_x) the same OH-initiated oxidation chemistry produces more hydroperoxides and fewer carbonyl products.⁶⁵ However, a scaling factor can be incorporated in the transformation rules if the branching ratios are known or can be estimated with *ab initio* methods. For the comparison with the ESI-based MS data, this is not a major limitation because there are no simple relationships between the detection efficiency in ESI and the concentration of the analyte species.⁶⁶

Applying COBRA to the simulation of oligomerization in isoprene OA is a good example of the utility of computational tools for understanding complex natural mixtures and verifying experimental data. An important strength of COBRA is its ability to handle a complex simulation and generate a large number of predicted compounds. While the combinatorial explosion of generated structures means computation time is currently on the order of several days, this time can be significantly reduced in future work by using parallel computing algorithms. If pertinent experimental data are available, direct comparison between the observed and predicted compounds can be made to better constrain chemistry and chemical structures. Furthermore, as COBRA reduces the number of possible structures available for a given chemical formula, the predicted structures may be useful for discriminating isobaric species in a mass spectrum. Applying a small set of transformation rules to predict an experimentally determined high-resolution mass spectrum may become a powerful tool for better understanding the chemistry of complex systems comprised of hundreds or thousands of individual compounds.

■ ASSOCIATED CONTENT

🔍 Supporting Information

Supporting Table 1: isoprene high-NO_x SOA high-resolution negative ion mode ESI-MS data, compared with molecular formulas predicted by COBRA. This material is available free of charge via the Internet at <http://pubs.acs.org>.

■ AUTHOR INFORMATION

Corresponding Author

*P.B.: phone: (949) 824-5809; e-mail: pfbaldi@ics.uci.edu.
S.N.: phone: (949) 824-1262; e-mail: nizkorod@uci.edu.

Author Contributions

†These authors contributed equally to this work.

Notes

The authors declare no competing financial interest.

■ ACKNOWLEDGMENTS

The initial support for this project came from a seed grant from the UCI Environmental Institute. T.B.N. and S.A.N. acknowledge additional support by the NSF grants ATM-0831518 and CHE-0909227. The work of D.F. and P.B. was supported in part by NIH grants LM010235-01A1 and 5T15LM007743 to P.B. and NSF grant MRI EIA-0321390 to P.B. J.L. and A.L. are supported by the intramural research and development program of the W. R. Wiley Environmental Molecular Sciences Laboratory (EMSL), a national scientific user facility sponsored by the Office of Biological and Environmental Research and located at PNNL. PNNL is operated for the U.S. Department of Energy by Battelle Memorial Institute under contract no. DE-AC06-76RL0 1830.

■ REFERENCES

- (1) Kanakidou, M.; Seinfeld, J. H.; Pandis, S. N.; Barnes, I.; Dentener, F. J.; Facchini, M. C.; Van Dingenen, R.; Ervens, B.; Nenes, A.; Nielsen, C. J.; Swietlicki, E.; Putaud, J. P.; Balkanski, Y.; Fuzzi, S.; Horth, J.; Moortgat, G. K.; Winterhalter, R.; Myhre, C. E. L.; Tsigaridis, K.; Vignati, E.; Stephanou, E. G.; Wilson, J. Organic aerosol and global climate modelling: a review. *Atmos. Chem. Phys.* **2005**, *5*, 1053–1123.
- (2) Seinfeld, J. H.; Pankow, J. F. Organic atmospheric particulate material. *Annu. Rev. Phys. Chem.* **2003**, *54*, 121–140.

- (3) Mauderly, J. L.; Chow, J. C. Health effects of organic aerosols. *Inhalation Toxicol.* **2008**, *20* (3), 257–288.
- (4) Poschl, U. Atmospheric aerosols: Composition, transformation, climate and health effects. *Angew. Chem., Int. Ed. Engl.* **2005**, *44* (46), 7520–7540.
- (5) Docherty, K. S.; Stone, E. A.; Ulbrich, I. M.; DeCarlo, P. F.; Snyder, D. C.; Schauer, J. J.; Peltier, R. E.; Weber, R. J.; Murphy, S. M.; Seinfeld, J. H.; Grover, B. D.; Eatough, D. J.; Jimenez, J. L. Apportionment of Primary and Secondary Organic Aerosols in Southern California during the 2005 Study of Organic Aerosols in Riverside (SOAR-1). *Environ. Sci. Technol.* **2008**, *42* (20), 7655–7662.
- (6) Andreae, M. O.; Rosenfeld, D. Aerosol-cloud-precipitation interactions. Part 1. The nature and sources of cloud-active aerosols. *Earth-Sci. Rev.* **2008**, *89* (1–2), 13–41.
- (7) Rudich, Y.; Donahue, N. M.; Mentel, T. F. Aging of organic aerosol: Bridging the gap between laboratory and field studies. *Annu. Rev. Phys. Chem.* **2007**, *58*, 321–352.
- (8) Jimenez, J. L.; Canagaratna, M. R.; Donahue, N. M.; Prevot, A. S. H.; Zhang, Q.; Kroll, J. H.; DeCarlo, P. F.; Allan, J. D.; Coe, H.; Ng, N. L.; Aiken, A. C.; Docherty, K. S.; Ulbrich, I. M.; Grieshop, A. P.; Robinson, A. L.; Duplissy, J.; Smith, J. D.; Wilson, K. R.; Lanz, V. A.; Hueglin, C.; Sun, Y. L.; Tian, J.; Laaksonen, A.; Raatikainen, T.; Rautiainen, J.; Vaattovaara, P.; Ehn, M.; Kulmala, M.; Tomlinson, J. M.; Collins, D. R.; Cubison, M. J.; Dunlea, E. J.; Huffman, J. A.; Onasch, T. B.; Alfarra, M. R.; Williams, P. I.; Bower, K.; Kondo, Y.; Schneider, J.; Drewnick, F.; Borrmann, S.; Weimer, S.; Demerjian, K.; Salcedo, D.; Cottrell, L.; Griffin, R.; Takami, A.; Miyoshi, T.; Hatakeyama, S.; Shimono, A.; Sun, J. Y.; Zhang, Y. M.; Dzepina, K.; Kimmel, J. R.; Sueper, D.; Jayne, J. T.; Herndon, S. C.; Trimborn, A. M.; Williams, L. R.; Wood, E. C.; Middlebrook, A. M.; Kolb, C. E.; Baltensperger, U.; Worsnop, D. R. Evolution of Organic Aerosols in the Atmosphere. *Science* **2009**, *326* (5959), 1525–1529.
- (9) Laskin, J.; Laskin, A.; Roach, P. J.; Slysz, G. W.; Anderson, G. A.; Nizkorodov, S. A.; Bones, D. L.; Nguyen, L. Q. High-Resolution Desorption Electrospray Ionization Mass Spectrometry for Chemical Characterization of Organic Aerosols. *Anal. Chem.* **2010**, *82* (5), 2048–2058.
- (10) Bones, D. L.; Henricksen, D. K.; Mang, S. A.; Gonsior, M.; Bateman, A. P.; Nguyen, T. B.; Cooper, W. J.; Nizkorodov, S. A. Appearance of strong absorbers and fluorophores in limonene-O₃ secondary organic aerosol due to NH₄⁺-mediated chemical aging over long time scales. *J. Geophys. Res.* **2010**, *115* (D5), D05203 DOI: 10.1029/2009jd012864.
- (11) De Haan, D. O.; Tolbert, M. A.; Jimenez, J. L. Atmospheric condensed-phase reactions of glyoxal with methylamine. *Geophys. Res. Lett.* **2009**, *36*, 5.
- (12) Nizkorodov, S. A.; Laskin, J.; Laskin, A. Molecular chemistry of organic aerosols through the application of high resolution mass spectrometry. *Phys. Chem. Chem. Phys.* **2011**, *13* (9), 3612–3629.
- (13) Laskin, A.; Smith, J. S.; Laskin, J. Molecular Characterization of Nitrogen-Containing Organic Compounds in Biomass Burning Aerosols Using High-Resolution Mass Spectrometry. *Environ. Sci. Technol.* **2009**, *43* (10), 3764–3771.
- (14) Schmitt-Kopplin, P.; Gelencsér, A.; Dabek-Zlotorzynska, E.; Kiss, G.; Hertkorn, N.; Harir, M.; Hong, Y.; Gebefügi, I. Analysis of the Unresolved Organic Fraction in Atmospheric Aerosols with Ultrahigh-Resolution Mass Spectrometry and Nuclear Magnetic Resonance Spectroscopy: Organosulfates As Photochemical Smog Constituents. *Anal. Chem.* **2010**, *82* (19), 8017–8026.
- (15) Baltensperger, U.; Chirico, R.; DeCarlo, P. F.; Dommen, J.; Gaeggeler, K.; Heringa, M. F.; Li, M.; Prévôt, A. S.; Alfarra, M. R.; Gross, D. S.; Kalberer, M. Recent developments in the mass spectrometry of atmospheric aerosols. *Eur. J. Mass. Spectrom.* **2010**, *16* (3), 389–395.
- (16) Kautzman, K. E.; Surratt, J. D.; Chan, M. N.; Chan, A. W. H.; Hersey, S. P.; Chhabra, P. S.; Dalleska, N. F.; Wennberg, P. O.; Flagan, R. C.; Seinfeld, J. H. Chemical Composition of Gas- and Aerosol-Phase Products from the Photooxidation of Naphthalene. *J. Phys. Chem. A* **2009**, *114* (2), 913–934.
- (17) Altieri, K. E.; Seitzinger, S. P.; Carlton, A. G.; Turpin, B. J.; Klein, G. C.; Marshall, A. G. Oligomers formed through in-cloud methylglyoxal reactions: Chemical composition, properties, and mechanisms investigated by ultra-high resolution FT-ICR mass spectrometry. *Atmos. Environ.* **2008**, *42* (7), 1476–1490.
- (18) Surratt, J. D.; Murphy, S. M.; Kroll, J. H.; Ng, N. L.; Hildebrandt, L.; Sorooshian, A.; Szmigielski, R.; Vermeylen, R.; Maenhaut, W.; Claeys, M.; Flagan, R. C.; Seinfeld, J. H. Chemical composition of secondary organic aerosol formed from the photooxidation of isoprene. *J. Phys. Chem. A* **2006**, *110* (31), 9665–9690.
- (19) Chan, A. W. H.; Chan, M. N.; Surratt, J. D.; Chhabra, P. S.; Loza, C. L.; Crouse, J. D.; Yee, L. D.; Flagan, R. C.; Wennberg, P. O.; Seinfeld, J. H. Role of aldehyde chemistry and NO_x concentrations in secondary organic aerosol formation. *Atmos. Chem. Phys.* **2010**, *10*, 7169–7188.
- (20) Nguyen, T. B.; Roach, P. J.; Laskin, J.; Laskin, A.; Nizkorodov, S. A. Effect of humidity on the composition of isoprene photooxidation secondary organic aerosol. *Atmos. Chem. Phys.* **2011**, *11*, 6931–6944.
- (21) Reinhardt, A.; Emmenegger, C.; Gerrits, B.; Panse, C.; Dommen, J.; Baltensperger, U.; Zenobi, R.; Kalberer, M. Ultrahigh mass resolution and accurate mass measurements as a tool to characterize oligomers in secondary organic aerosols. *Anal. Chem.* **2007**, *79* (11), 4074–4082.
- (22) Nguyen, T. B.; Laskin, J.; Laskin, A.; Nizkorodov, S. A. Nitrogen containing organic compounds and oligomers in secondary organic aerosol formed by photooxidation of isoprene. *Environ. Sci. Technol.* **2011**, *45*, 6908–6918.
- (23) Tolocka, M. P.; Jang, M.; Ginter, J. M.; Cox, F. J.; Kamens, R. M.; Johnston, M. V. Formation of oligomers in secondary organic aerosol. *Environ. Sci. Technol.* **2004**, *38* (5), 1428–1434.
- (24) Barsanti, K. C.; Pankow, J. F. Thermodynamics of the formation of atmospheric organic particulate matter by accretion reactions - 2. Dialdehydes, methylglyoxal, and diketones. *Atmos. Environ.* **2005**, *39* (35), 6597–6607.
- (25) Barsanti, K. C.; Pankow, J. F. Thermodynamics of the formation of atmospheric organic particulate matter by accretion reactions - Part 3: Carboxylic and dicarboxylic acids. *Atmos. Environ.* **2006**, *40* (34), 6676–6686.
- (26) Hamilton, J. F.; Lewis, A. C.; Carey, T. J.; Wenger, J. C. Characterization of polar compounds and oligomers in secondary organic aerosol using liquid chromatography coupled to mass spectrometry. *Anal. Chem.* **2008**, *80* (2), 474–480.
- (27) Chan, M. N.; Surratt, J. D.; Claeys, M.; Edgerton, E. S.; Tanner, R. L.; Shaw, S. L.; Zheng, M.; Knipping, E. M.; Eddingsaas, N. C.; Wennberg, P. O.; Seinfeld, J. H. Characterization and Quantification of Isoprene-Derived Epoxydiols in Ambient Aerosol in the Southeastern United States. *Environ. Sci. Technol.* **2010**, *44* (12), 4590–4596.
- (28) Yasmeen, F.; Sauret, N.; Gal, J.-F.; Maria, P.-C.; Massi, L.; Maenhaut, W.; Claeys, M. Characterization of oligomers from methylglyoxal under dark conditions: a pathway to produce secondary organic aerosol through cloud processing during nighttime. *Atmos. Chem. Phys.* **2010**, *10* (8), 3803–3812.
- (29) Garland, R. M.; Elrod, M. J.; Kincaid, K.; Beaver, M. R.; Jimenez, J. L.; Tolbert, M. A. Acid-catalyzed reactions of hexanal on sulfuric acid particles: identification of reaction products. *Atmos. Environ.* **2006**, *40* (35), 6863–6878.
- (30) Jang, M.; Carroll, B.; Chandramouli, B.; Kamens, R. M. Particle Growth by Acid-Catalyzed Heterogeneous Reactions of Organic Carbonyls on Preexisting Aerosols. *Environ. Sci. Technol.* **2003**, *37* (17), 3828–3837.
- (31) Jang, M. S.; Czoschke, N. M.; Northcross, A. L. Semiempirical model for organic aerosol growth by acid-catalyzed heterogeneous reactions of organic carbonyls. *Environ. Sci. Technol.* **2005**, *39* (1), 164–174.
- (32) Chen, J. H.; Baldi, P. No Electron Left Behind: A Rule-Based Expert System To Predict Chemical Reactions and Reaction Mechanisms. *J. Chem. Inf. Model.* **2009**, *49* (9), 2034–2043.
- (33) Kayala, M. A.; Azencott, C. A.; Chen, J. H.; Baldi, P. Learning to predict chemical reactions. *J. Chem. Inf. Model.* **2011**, *51* (9), 2209–22.

- (34) Weininger, D. SMILES, a chemical language and information system. 1. Introduction to methodology and encoding rules. *J. Chem. Inf. Comput. Sci.* **1988**, *28* (1), 31–36.
- (35) *Daylight Theory Manual*, Daylight Chemical Information Systems, Inc., release date August 1, 2011. <http://www.daylight.com/dayhtml/doc/theory/index.html>.
- (36) OpenEye Scientific Software, I., OEChem, version 1.7.4. In *OpenEye Scientific Software*: Santa Fe, NM, USA, 2010.
- (37) Kim, S.; Rodgers, R. P.; Marshall, A. G. Truly “exact” mass: Elemental composition can be determined uniquely from molecular mass measurement at <0.1 mDa accuracy for molecules up to <500 Da. *Int. J. Mass Spectrom.* **2006**, *251* (2–3), 260–265.
- (38) Carlton, A. G.; Wiedinmyer, C.; Kroll, J. H. A review of secondary organic aerosol formation from isoprene. *Atmos. Chem. Phys.* **2009**, *9* (14), 4987–5005.
- (39) Edney, E. O.; Kleindienst, T. E.; Jaoui, M.; Lewandowski, M.; Offenber, J. H.; Wang, W.; Claeys, M. Formation of 2-methyl tetrols and 2-methylglyceric acid in secondary organic aerosol from laboratory irradiated isoprene/NO_x/SO₂/air mixtures and their detection in ambient PM_{2.5} samples collected in the eastern United States. *Atmos. Environ.* **2005**, *39* (29), 5281–5289.
- (40) Grosjean, D.; Williams, E. L.; Grosjean, E. Atmospheric chemistry of isoprene and of its carbonyl products. *Environ. Sci. Technol.* **1993**, *27* (5), 830–840.
- (41) Spaulding, R. S.; Schade, G. W.; Goldstein, A. H.; Charles, M. J. Characterization of secondary atmospheric photooxidation products: Evidence for biogenic and anthropogenic sources. *J. Geophys. Res.* **2003**, *108* (D8), 4247 DOI: 10.1029/2002jd002478.
- (42) Kleindienst, T. E.; Lewandowski, M.; Offenber, J. H.; Jaoui, M.; Edney, E. O. The formation of secondary organic aerosol from the isoprene plus OH reaction in the absence of NO_x. *Atmos. Chem. Phys.* **2009**, *9* (17), 6541–6558.
- (43) Claeys, M.; Graham, B.; Vas, G.; Wang, W.; Vermeylen, R.; Pashynska, V.; Cafmeyer, J.; Guyon, P.; Andreae, M. O.; Artaxo, P.; Maenhaut, W. Formation of secondary organic aerosols through photooxidation of isoprene. *Science* **2004**, *303* (5661), 1173–1176.
- (44) Paulot, F.; Crounse, J. D.; Kjaergaard, H. G.; Kroll, J. H.; Seinfeld, J. H.; Wennberg, P. O. Isoprene photooxidation: new insights into the production of acids and organic nitrates. *Atmos. Chem. Phys.* **2009**, *9*, 1479–1501.
- (45) Szmigielski, R.; Surratt, J. D.; Vermeylen, R.; Szmigielska, K.; Kroll, J. H.; Ng, N. L.; Murphy, S. M.; Sorooshian, A.; Seinfeld, J. H.; Claeys, M. Characterization of 2-methylglyceric acid oligomers in secondary organic aerosol formed from the photooxidation of isoprene using trimethylsilylation and gas chromatography/ion trap mass spectrometry. *J. Mass Spectrom.* **2007**, *42* (1), 101–116.
- (46) Tan, Y.; Carlton, A. G.; Seitzinger, S. P.; Turpin, B. J. SOA from methylglyoxal in clouds and wet aerosols: Measurement and prediction of key products. *Atmos. Environ.* **2010**, *44* (39), 5218–5226.
- (47) Petitjean, M.; Reyes-Perez, E.; Perez, D.; Mirabel, P.; Le Calve, S. Vapor Pressure Measurements of Hydroxyacetaldehyde and Hydroxyacetone in the Temperature Range (273 to 356) K. *J. Chem. Eng. Data* **2009**, *55* (2), 852–855.
- (48) Healy, R. M.; Wenger, J. C.; Metzger, A.; Duplissy, J.; Kalberer, M.; Dommen, J. Gas/particle partitioning of carbonyls in the photooxidation of isoprene and 1,3,5-trimethylbenzene. *Atmos. Chem. Phys.* **2008**, *8* (12), 3215–3230.
- (49) Liggio, J.; Li, S. M.; McLaren, R. Reactive uptake of glyoxal by particulate matter. *J. Geophys. Res., [Atmos.]* **2005**, *110* (D10), D10304.
- (50) Liggio, J.; Li, S.-M.; McLaren, R. Heterogeneous reactions of glyoxal on particulate matter: identification of acetals and sulfate esters. *Environ. Sci. Technol.* **2005**, *39* (6), 1532–1541.
- (51) Zhao, J.; Levitt, N. P.; Zhang, R.; Chen, J. Heterogeneous reactions of methylglyoxal in acidic media: implications for secondary organic aerosol formation. *Environ. Sci. Technol.* **2006**, *40* (24), 7682–7687.
- (52) Bateman, A. P.; Walser, M. L.; Desyaterik, Y.; Laskin, J.; Laskin, A.; Nizkorodov, S. A. The Effect of Solvent on the Analysis of Secondary Organic Aerosol Using Electrospray Ionization Mass Spectrometry. *Environ. Sci. Technol.* **2008**, *42* (19), 7341–7346.
- (53) Witz, G. Biological interactions of alpha,beta-unsaturated aldehydes. *Free Radical Biol. Med.* **1989**, *7* (3), 333–349.
- (54) Wynder, E. L.; Hoffmann, D. Tobacco and Health. *N. Engl. J. Med.* **1979**, *300* (16), 894–903.
- (55) Berhane, K.; Widersten, M.; Engstrom, A.; Kozarich, J. W.; Mannervik, B. Detoxication of base propenals and other alpha, beta-unsaturated aldehyde products of radical reactions and lipid peroxidation by human glutathione transferases. *Proc. Natl. Acad. Sci. U.S.A.* **1994**, *91* (4), 1480–1484.
- (56) Trombetta, D.; Saija, A.; Bisignano, G.; Arena, S.; Caruso, S.; Mazzanti, G.; Uccella, N.; Castelli, F. Study on the mechanisms of the antibacterial action of some plant alpha,beta-unsaturated aldehydes. *Letts. Appl. Microbiol.* **2002**, *35* (4), 285–290.
- (57) Lambert, C.; McCue, J.; Portas, M.; Ouyang, Y.; Li, J.; Rosano, T. G.; Lazis, A.; Freed, B. M. Acrolein in cigarette smoke inhibits T-cell responses. *J. Allergy Clin. Immunol.* **2005**, *116* (4), 916–922.
- (58) Andre, E.; Campi, B.; Materazzi, S.; Trevisani, M.; Amadesi, S.; Massi, D.; Creminon, C.; Vaksman, N.; Nassini, R.; Civelli, M.; Baraldi, P. G.; Poole, D. P.; Bunnett, N. W.; Geppetti, P.; Patacchini, R. Cigarette smoke-induced neurogenic inflammation is mediated by alpha,beta-unsaturated aldehydes and the TRPA1 receptor in rodents. *J. Clin. Invest.* **2008**, *118* (7), 2574–2582.
- (59) Kehrer, J. P.; Biswal, S. S. The molecular effects of acrolein. *Toxicol. Sci.* **2000**, *57* (1), 6–15.
- (60) Rohr, A. C.; Shore, S. A.; Spengler, J. D. Repeated exposure to isoprene oxidation products causes enhanced respiratory tract effects in multiple murine strains. *Inhalation Toxicol.* **2003**, *15* (12), 1191–1207.
- (61) Delfino, R.; Sioutas, J.; Malik, C. S., Potential role of ultrafine particles in associations between airborne particle mass and cardiovascular health. *Environ. Health Perspect.* **2005**, *113* (8), 934–46.
- (62) Dockery, D. W.; Pope, C. A., 3rd; Xu, X.; Spengler, J. D.; Ware, J. H.; Fay, M. E.; Ferris, B. G., Jr.; Speizer, F. E. An association between air pollution and mortality in six U.S. cities. *N. Engl. J. Med.* **1993**, *329* (24), 1753–9.
- (63) Pope, C. A., III; Burnett, R. T.; Thun, M. J.; Calle, E. E.; Krewski, D.; Ito, K.; Thurston, G. D. Lung cancer, cardiopulmonary mortality, and long-term exposure to fine particulate air pollution. *J. Am. Med. Assoc.* **2002**, *287* (9), 1132–1141.
- (64) Samet, J. M.; Dominici, F.; Currier, I.; Coursac, I.; Zeger, S. L. Fine particulate air pollution and mortality in 20 U.S. cities, 1987–1994. *N. Engl. J. Med.* **2000**, *343* (24), 1742–1749.
- (65) Atkinson, R. Atmospheric chemistry of VOCs and NO_x. *Atmos. Environ.* **2000**, *34* (12–14), 2063–2101.
- (66) Tang, K.; Page, J. S.; Smith, R. D. Charge competition and the linear dynamic range of detection in electrospray ionization mass spectrometry. *J. Am. Soc. Mass Spectrom.* **2004**, *15* (10), 1416–1423.